BUTTERWORTH HEINEMANN

Laminar cooling of pseudoplastic fluids flowing through cylindrical horizontal pipes

I. Azevedo, M. Lebouche and R. Devienne
LEMTA.URA875.NANCY I, Vandoeuvre-lès-Nancy, France

We present results concerning heat transfer for pseudoplastic fluids flowing inside cylindrical tubes. The fluids are cooled by an external turbulent counterflow of water. A method is developed to evaluate the values of the local heat exchange coefficients. The variations of the associated Nusselt numbers can be approached using the dimensionless axial abscissa $X_+ = (2z/D)/\mathrm{Pe}$. Experimentation shows that the Nusselt numbers remain slightly dependent on the difference between the inlet temperature of the pseudoplastic fluid T_e and the wall temperatures $T_w(z)$. This last phenomenum, attributed to the variations of consistency K and rheological index n with temperature, can be linked to the evolutions of the axial velocity profiles, experimentally determined by laser Doppler anemometry. A very simple correlation $\mathrm{Nu}(z) = 1.15\{(3n+1)/(4n)\}^{1/3}\{1 - 0.008[T_e - T_w(z)]\}\, X_+^{-0.36}$ seem to be acceptable in our experimental range. Comparisons with numerical predictions are also proposed.

Keywords: cooling; pseudoplastic; fluids; thermodependency; laminar; pipe

Introduction

It is well known that the design of heat exchangers is not a trivial operation when non-Newtonian fluids are involved. This problem primarily concerns food or chemical industries wherein products to be treated may exhibit complex rheological behavior. Moreover, such fluids as tomato sauces and fruit purees generally present high apparent viscosity so that situations appear for which the thermal regime is never established inside the exchanger. This remark is valuable for the case of cooling, with an increasing complexity. Planners of thermal plants can find many studies in the literature that consider both theoretical and experimental approaches. See, for example, the following papers: Oliver and Jenson (1964), Christiansen et al. (1966), Forest and Wilkinson (1977), Popovska and Wilkinson (1977). These authors attempt to analyze the effect of such phenomena as:

(1) thermodependency, also extensively treated in the case of heating, see for example, Sieder and Tate (1936), Metzner et al. (1957), Joshi and Bergles (1982);
(2) viscous dissipation, which can play an important role in cooling processes because in these situations the energy transfer is generally weak; and
(3) natural convection.

We present some results concerning the heat transfer coefficients between a pseudoplastic fluid, called the *working fluid*, and a tube wall cooled by a Newtonian fluid. The tested geometry corresponds to counterflows inside a horizontal tube for the working fluid and inside an external concentric annular space for the cooling fluid. Because the heat flux density cannot be considered here as a constant, it follows that the wall temperature seems to vary along the tube. This study may provide practical results concerning the shell and tube heat exchanger.

Experimental details

Experimental installation. This is essentially a system allowing the flow of a "hot" fluid in a closed loop (see Figure 1). This flow is generated by a helicoidal pump, which is chosen to avoid excessive shear. An initial tube section of 47 diameters is left at the beginning, which allows the settling of the velocity profile for any flow rates, these being

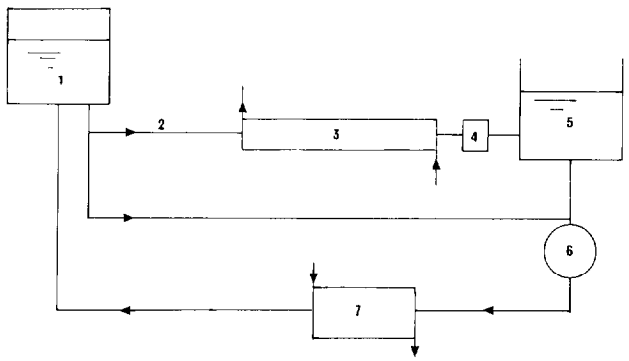

Figure 1 Schematic of the experimental apparatus

Address reprint requests to Prof. R. Devienne, LEMTA/ENSEM, 2 Avenue de la Forêt de Haye, BP 160, 54504 Vandoeuvre-lès-Nancy, Cedex, France.

Received 30 July 1993; accepted 10 July 1994

Int. J. Heat and Fluid Flow 16: 125–130, 1995

655 Avenue of the Americas, New York, NY 10010

SSDI 0142-727X/95/$10.00
SSDI 0142-727X(94)00013-3

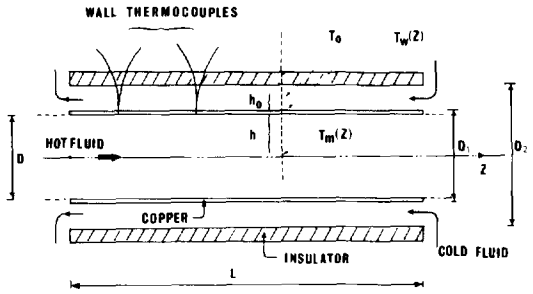

Figure 2 Details of the tested zone

measured by an electromagnetic flowmeter. The hydrodynamic establishing length can be evaluated from the formula $L/D \approx Re_g/10$ and, in fact, our very consistent products lead to low Reynolds numbers (< 20) so that the velocity field develops very quickly. The mean input temperature T_e can be controlled by a heat exchanger, and it is measured by a thermocouple to within ± 0.1°C. The observed region comprises essentially a horizontal copper tube of $L = 3.2$ m in length, through which flows the hot liquid (see Figure 2). About 40 thermocouples have been inserted into the 2.5-mm thick wall, which are then connected to a central unit, some of these are fixed up and down for the same section to control the eventual occurring of natural convection. The external cooling liquid (a mixture of water and ethyl glycol) flows in an annular section ($D_1 = 35$ mm, $D_2 = 72$ mm) surrounding the tube. Because of the chemical composition, the mean inlet temperature of the cooling fluid may be as low as -10°C. The entrance and the exit of the fluid is ensured by three radial guides. The mean inlet and outlet temperatures of the cold liquid are measured by thermometers with platinum probes capable of measuring these typically small temperature differences. Measuring the flow rate of this cold liquid allows us to estimate the total power exchanged. In fact, the mean inlet temperature and the flow rate remain constant (see Table 1, which also indicates the principal characteristics of the installation).

The axial velocity profiles at the entrance and at the exit are measured by a laser Doppler anemometer.

Table 1 Main characteristics of the installation

Inside diameter of the tube	$D = 0.034$ m
Length of the cooling zone	$106 \cdot D$
Flow rate for the hot fluid	$Q = 0 \rightarrow 2.2$ m^3/h
Average velocity	$V_d = 0 \rightarrow 0.47$ m/s
Total power exchanged	$\Phi = 0 \rightarrow 3.1$ kw
Number of wall temperature probes	41 k-thermocouples
Reynolds number	$0 \rightarrow 20$
Flow rate for the cooling fluid	2.2 m^3/h
Inlet temperature for the hot fluid	$18 \rightarrow 52$°C
Inlet temperature for the cold fluid	-6.5°C

Tested fluids. We used water solutions of carboxymethylcellulose (c.m.c) with a concentration of 4 percent in weight. We also added a few hundred p.p.m. of sodium (ethyl mercurithio)$^{-2}$ benzoate in order to prevent bacteriological degradation. The rheological behavior was measured by means of a stress-controlled rheometer equipped with a plate and cone geometry (diameter = 4 cm, angle = 4°). The diagrams of Figure 3 show clearly that the power law $\tau = K\dot{\gamma}^n$ can only be applied in certain ranges of the shear rate $\dot{\gamma}$, which are to be specified—an exact power law would correspond to straight lines. In the present situation, we restrict ourselves to the range 10–150 s^{-1}, which are the bounds of the values considered in our experiment. We recall that the wall shear rate $\dot{\gamma}_w$ is the main parameter governing heat transfer.

The dependence on the temperature of both the consistency K and the rheological index n was accurately measured (see Figure 4). In the temperature domain considered here, the exponential law seems to be sufficient (see Figure 4), that is: $K = a \exp(-b\,T) = 42.2 \exp(-0.049\,T)$; $n = a' \exp(b'\,T) = 0.43 \exp(0.0096\,T)$. Note that, contrary to the usual case, in this study, it is necessary to account for the variation of n with temperature, because the shape of the velocity profiles at the entrance depends on the index n (see *Comparison with numerical results* subsection).

Evaluation of the local exchange coefficients. The exchange coefficient for the pseudoplastic fluid $h = h(z)$ is defined by: $h(z) = \varphi(z)/\{T_m(z) - T_w(z)\}$; where $\varphi(z)$ denotes the local heat flux density for the inner surface of the copper tube. $T_m(z)$, $T_w(z)$ are, respectively, the mean and wall

Notation

a, b	constants for the expression of the consistency
a', b'	constants for the power law index
C_p, C_{p0}	specific heats (working fluid and cold fluid)
D, D_1, D_2	diameters
e	ice thickness
$Gz = \pi/4\ Pe/z/D$	Graetz number
$h(z)$, h_0	heat exchange coefficients
K	consistency
L	length of the exchange zone
n	power law index
Nu, Nu'	Nusselt numbers
$Pe = \rho\, V_d\, DC_p/\lambda$	Peclet number
Q, Q_0	flow rates (working fluid and cold fluid)
$Re_g = 1/\Delta^n\ \rho\ V_d^{2-n} D^n/8^{n-1}\ K$	generalized Reynolds number
T	temperature, °C
$T_e = T_m(0)$	inlet temperature (working fluid)
$T_m(z)$, $T_0(z)$	mean temperatures for the hot and cold fluids
$T_{o,0}$, $T_{i,0}$	outlet, inlet mean temperatures (cold fluid)
$T_w(z)$	wall temperatures
V, V_d	local, mean axial velocities
$X_+ = 2\ z/D\ Pe$	dimensionless axial abscissa
z, z'	axial abscissae
Greek	
$\dot{\gamma}$	shear rate
λ, λ_g	thermal conductivity
ρ	density
τ	shear stress
ϕ	total exchanged power
φ, φ'	heat flux densities
$\Delta = 3n + 1/4n$	wall shear rate correction

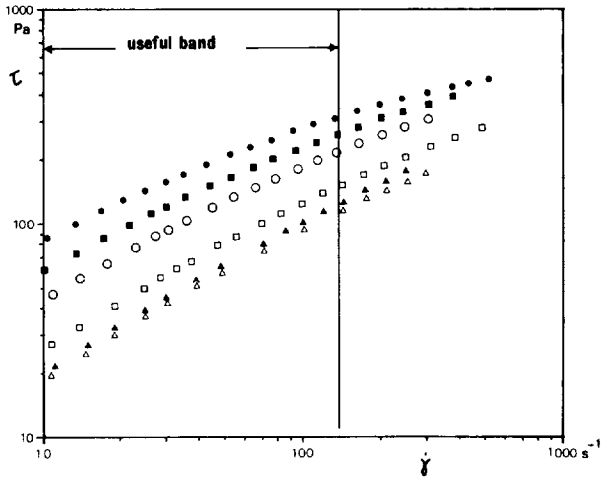

Figure 3 Variations of the shear stress τ versus the shear rate $\dot{\gamma}$ for different temperatures (● 2°C; ■ 10°C; ○ 20°C; □ 30°C; ▲ 40°C; △ 50°C)

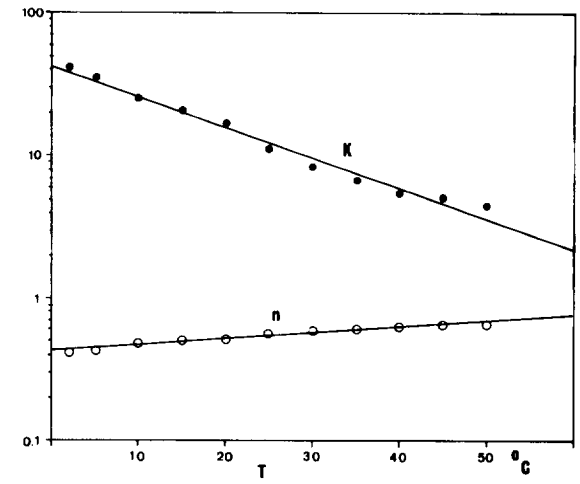

Figure 4 Evolution of the consistency K and of the index n with temperature (● K ($Pa \cdot s^n$); ○ n)

temperatures (see Figure 2) with

$$T_m(z) = T_e + \frac{1}{\rho \cdot C_p \cdot Q} \int_0^z \varphi(z') \cdot \pi \cdot D \cdot dz'$$

For the external cooling fluid, we can write $h_0 = \varphi'(z)/\{T_w(z) - T_0(z)\}$, $\varphi'(z)$ being the local heat flux density for the outer surface of the copper tube.

The axial heat flux inside the wall may be neglected, so that $D_1 \cdot \varphi'(z) = D \cdot \varphi(z)$. Here, $T_0(z)$ is the mean temperature of the cooling fluid. This leads to $h(z) = h_0 \cdot (D_1/D) \cdot [T_w(z) - T_0(z)]/[T_m(z) - T_w(z)]$. The cooling fluid undergoes only small variations of temperature—see the following paragraph, for instance, and because the flow regime is turbulent, the h_0 coefficient may be assumed to be constant along the tube and can be estimated from an energy balance on the total exchanged power ϕ:

$$\phi = \int_0^L \varphi'(z) \cdot \pi \cdot D_1 \cdot dz = h_0 \int_0^L \{T_w(z) - T_0(z)\} \pi \cdot D_1 \cdot dz$$

with $\phi = \rho \cdot C_{p0} \cdot Q_0 \cdot (T_{o,0} - T_{i,0})$, obtained by a heat balance on the cooling water. Here Q_0, $T_{o,0}$, $T_{i,0}$ are, respectively, the flow rate and the outlet and inlet temperatures for the cooling fluid: $T_{o,0} = T_0(0)$, $T_{i,0} = T_0(L)$. The results are represented by means of the local Nusselt number, defined as $Nu = h \cdot D/\lambda$. λ, the thermal conductivity, being taken as equal to that of water.

Validation of the procedure and precision. The use of water as the inner fluid may produce some validation of the procedure proposed above. Figure 5 shows the evolution of the wall temperature T_w versus z, for the following experimental conditions $T_e = 19.3$°C, $T_{o,0} = 3.85$°C, $T_{i,0} = 3.15$°C, $Q = 1.75\ 10^{-4}$ m³/s, $Q_0 = 4.4\ 10^{-4}$ m³/s. This evolution may be simply approximated by a linear relation $T_w = 15\text{–}1.5(z/L)$. For this particular situation and due to the flow regime, the low values of the temperatures differences and also the noticeable value of the total heat flux ϕ compel us to account for the variations of T_m with the abscissa z. We propose $T_m(z) \simeq T_e + \phi/\rho \cdot C_p \cdot Q \cdot z/L$. An identical approximation may be used for T_0, $T_0 \simeq T_{o,0} + (T_{i,0} - T_{o,0}) \cdot (z/L)$. First, the determination of the h_0 coefficient leads to $h_0 = 309$ W/(m² · °C), a calculation of this coefficient based on the Chilton–Colburn correlation used with a hydraulic diameter $(D_1 + D_2)/2$ produces a predicted value about 332 W/(m² · °C). Second, the ratio $(T_w - T_0)/(T_m - T_w)$ may be expressed as a function of z. It is important to notice that this quantity varies only very weakly with z: $2.59 < (T_w - T_0)/(T_m - T_w) < 2.54$. A mean value of this ratio corresponds to $h = 936$ W/(m² · °C). The same correlation as before would give $h = 1024$ W/(m² · °C).

The most important term in the relative precision formula for the Nusselt numbers may be written as follows:

$$\Delta Nu/Nu = (\Delta\phi/\phi + \Delta T_w)(1/T_w - T_0 + 1/T_m - T_w) + \Delta T_0/(T_w - T_0) + \Delta T_m/(T_m - T_w)$$

$$\Delta\phi/\phi = \Delta(T_{o,0} - T_{i,0}/(T_{o,0} - T_{i,0})$$

$$\Delta T_m = \Delta T_e + z/L \cdot \Delta\phi/(\rho \cdot C_p \cdot Q)$$

$$\Delta T_0 = \Delta T_{o,0} + z/L \cdot \Delta\phi/(\rho \cdot C_p \cdot Q_0)$$

where it is assumed that random errors in the integrand will cancel. Generally, when pseudoplastic solutions are tested, the first term is preponderant, and it is the reason why a high-precision thermometer has been used for the determination of $T_{o,0}$ and $T_{i,0}$. Furthermore, for the determination of $T_w - T_0$ and $T_m - T_0$, it seems to be possible, without loss of precision, to replace T_m and T_0 by T_e and $T_{i,0}$ because the temperature differences are important enough and the heat flux sufficiently weak. Nevertheless, we cannot hope for a precision better than 15 percent induced by $\Delta T_w = \Delta T_e = 0.2$°C, $\Delta(T_{i,0} - T_{o,0}) = 0.02$°C.

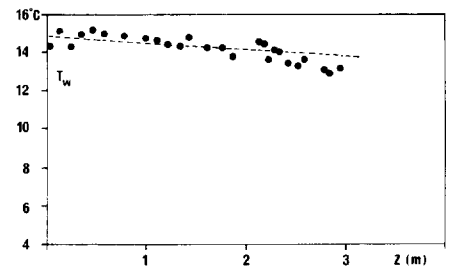

Figure 5 Validation case: T_w versus abscissa z [$T_e = 19.3$°C; $T_{i,0} = 3.15$°C; $\phi = 1260$ W; Reynolds numbers 7,500 and 2,000 (inner and outer flows)—$T_w = 15\text{–}1.5(z/L)$]

Experimental results

Thermal exchanges. Figure 6 illustrates an example of the wall temperature evolution; these variations seem to be large; moreover, it is possible to distinguish a decrease of slope when the temperature falls below the freezing point. Figure 7 gives an example of the variations in the Nusselt numbers, and clearly indicates that we are in a situation where the thermal field is not established and far from an asymptotic behavior. We can account for the variations of the axial position and of the flow rate by using the usual variable $X_+ = 2 \cdot z/(D \cdot \mathrm{Pe})$, a dimensionless axial abscissa (see Figure 8). Note that the Pe number does not contain information about the rheological behavior and that this analysis remains reasonable for all the values of the inlet temperatures T_e.

On the other hand, it should be noted that the variations in the Nusselt number remain dependent on this inlet

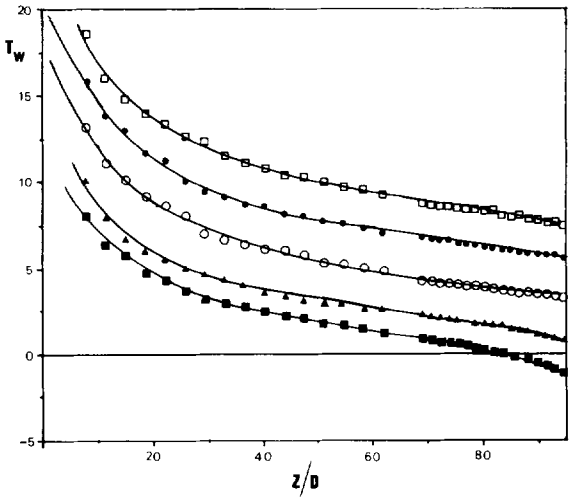

Figure 6 Wall temperature T_w versus reduced abscissa z/D for different flow rates and a constant mean in going tempera ture $T_e = 35°C$ (□ 1,200 1/h $Re_g = 12.1$; ● 750 1/h $Re_g = 6.2$; ○ 450 1/h $Re_g = 3.1$; ▲ 150 1/h $Re_g = 0.7$; ■ 75 1/h $Re_g = 0.2$)

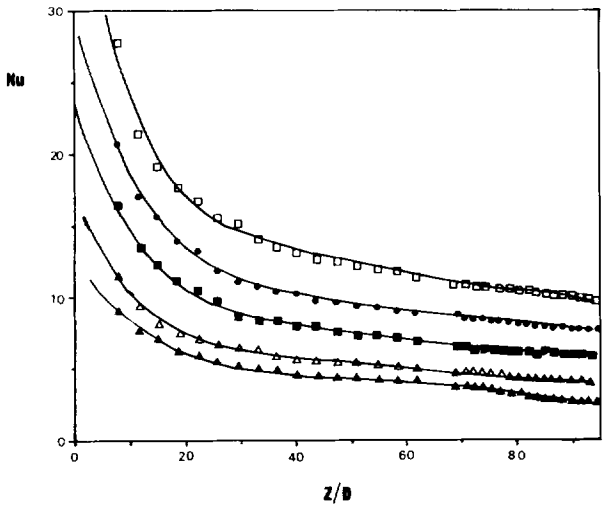

Figure 7 Nusselt number Nu versus axial abscissa z/D for different flow rates and a constant mean ingoing temperature $T_e = 52°C$ (□ 1.200 1/h $Re_g = 18.7$; ● 750 1/h $Re_g = 10$; ■ 450 1/h $Re_g = 5.2$; △ 150 1/h $Re_g = 1.3$; ▲ 75 1/h $Re_g = 0.5$)

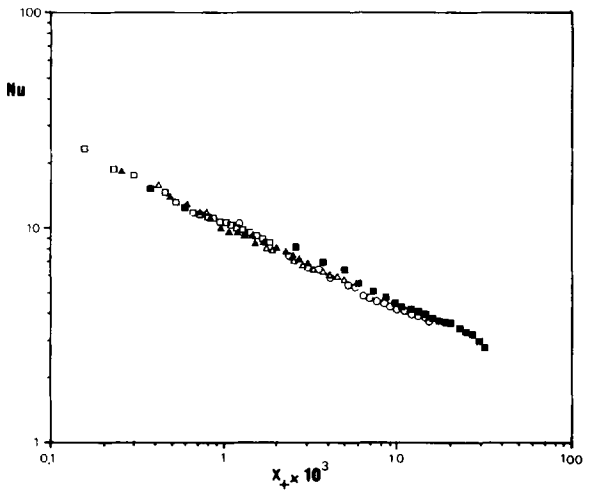

Figure 8 Nusselt number Nu versus $X_+ = 2z/D/\mathrm{Pe}$ (logarithmic representation) for a constant mean ingoing temperature $T_e = 52°C$ (□ 1,200 1/h $Re_g = 18.7$; ▲ 750 1/h $Re_g = 10$; ○ 150 1/h $Re_g = 1.3$; ■ 75 1/h $Re_g = 0.5$)

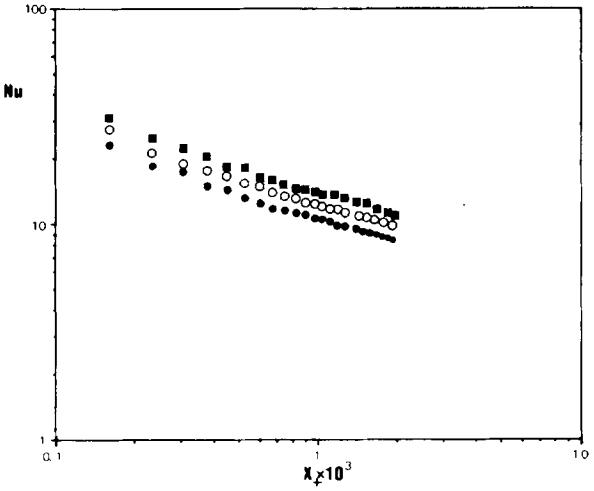

Figure 9 Nusselt number versus $X_+ = 2z/D/\mathrm{Pe}$ (logarithmic representation) for different mean ingoing temperatures T_e and a fixed flow rate (1,200 1/h) ■ $T_e = 52°C$, $n = 0.68$; ○ $T_e = 35°C$; $n = 0.60$; ● $T_e = 18°C$; $n = 0.51$

temperature T_e (see Figure 9). This effect can be attributed to the thermodependency. The value of the exponent of X_+ has been found to be 0.36, this being the mean value of all the experimental points. It is, nevertheless, fairly close to the value of 1/3 found in the work of Levêque, $\mathrm{Nu} = 1.41\,(\mathrm{Gz})^{1/3}$.

The model. As usual, the correlation above is adjusted by multiplying it by two correcting factors. The first factor, written as $\Delta^{1/3} = \{(3n + 1)/(4n)\}^{1/3}$ describes the non-Newtonian character of the fluid and was introduced by Pigford (1955). To obtain a practical formula, we have chosen n to correspond to the inlet temperature. This correction is at most 7 percent, which is, therefore, insufficient to re-group all the Nusselt curves into one. This is explained by the fact that the negative effect ($T_e\uparrow$, $n\uparrow$, $\dot{\gamma}_w\downarrow$) adds to another negative effect caused by the progressive increase of the apparent viscosity. This increase is caused by

the cooling along the wall, which leads to a change in the wall shear rate (as shown later in subsection *Comparison with numerical results*). This change becomes *larger* as *the inlet temperature T_e increases.*

A second factor, therefore, becomes necessary, which is related to the wall temperature variations and more specifically to the thermodependency. Hence, we have chosen to write this correction as $1 + A \cdot [T_e - T_w(z)]$ (because this factor must tend to 1 for $T_e \simeq T_w(z)$). The constant A has been chosen to group all the 450 experimental points within a band of 10 percent in width (see Figure 10). It must be observed that if we introduce in A the parameter b corresponding to the variation of K with temperature, the above correction can still be written as follows:

$$1 + A \cdot [T_e - T_w(z)] = 1 - b \cdot \alpha \cdot [T_e - T_w(z)$$
$$\simeq \{\exp - b \cdot [T_e - T_w(z)]\}^{\alpha} = (Ke/K_w)^{\alpha}.$$

Therefore, we get a formulation similar to that of authors working on problems of the same type. See, for example, Metzner and Gluck (1959), Mizushina et al. (1967), Mahalingham et al. (1975). The value of the exponent α ($\alpha = 0.16$) is very close to that found in the correction of Sieder–Tate written as $(\mu_b/\mu_w)^{0.14}$, where μ_b is the viscosity evaluated at the average of the mean inlet and outlet temperatures, and μ_w the viscosity at the wall temperature. Nevertheless, the universality of the α constant is a daring assumption, and it should be verified by varying the parameter b.

Hence, we propose $\mathrm{Nu}(z) = 1.15\,[(3n + 1)/(4n)]^{1/3}\{1 - 0.008\,[T_e - T_w(z)]\}X_+^{-0.36}$ with the following validity conditions: $b \approx 0.05\ (^\circ\mathrm{C})^{-1}$, $10^{-4} < X_+ < 2\,10^{-2}$, $T_w > 0^\circ\mathrm{C}$. Note that in this correlation, it would be possible to numerically replace T_e by T_m, but while T_m varies significantly due to T_e, it does not change much along the axial coordinate.

Comparison with numerical results. We have used a numerical code presented elsewhere by El Ouardighi et al. (1989), which solves the coupled equations of the dynamical and thermal fields, and accounts for the variations of the parameters with temperature. It has been possible to introduce the distribution of wall temperatures resulting from the experiments. In this case, the code provides the local heat flux density $\varphi(z)$. A comparison can then be done with the

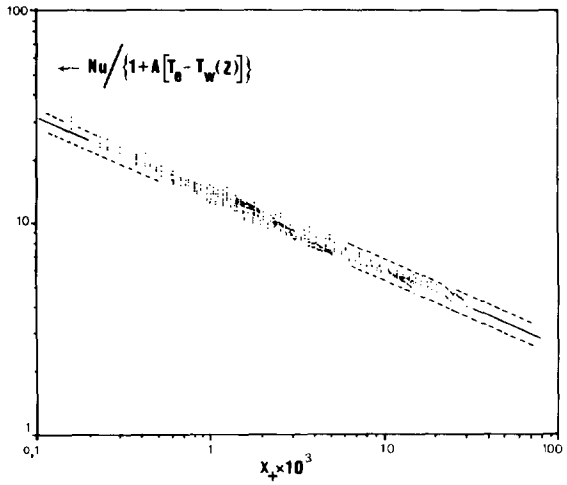

Figure 10 Global variations of the corrected Nusselt number $\mathrm{Nu}/\{1 + A[T_e - T_w(z)]\}$ versus $X_+ = 2z/D/\mathrm{Pe}$; · all experimental points; — proposed correlation (slope −0.36); - - - = 10 percent width band

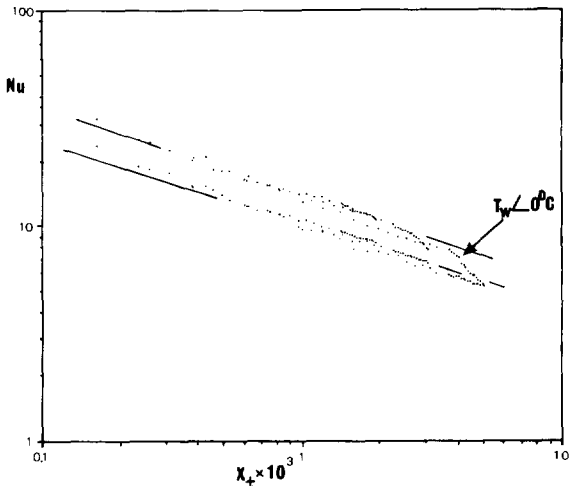

Figure 11 Comparison between experimental and numerical results; · experimental points; — numerical curves (upper one $T_e = 52^\circ\mathrm{C}$, lower one $T_e = 18^\circ\mathrm{C}$)

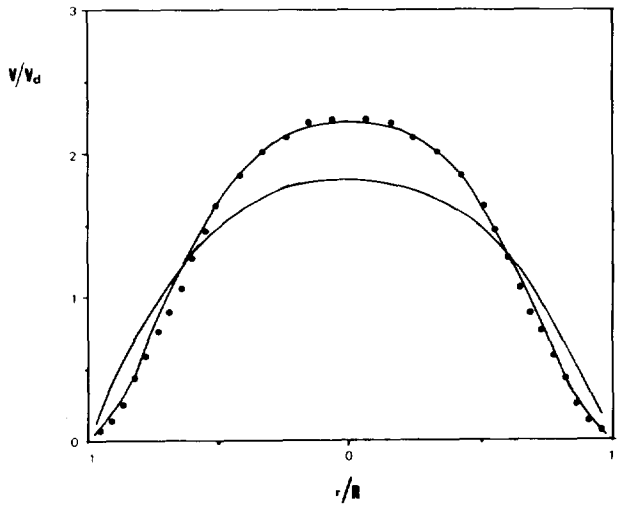

Figure 12 Axial velocity V/V_d evolution (for $T_e = 35^\circ\mathrm{C}$, 1,200 l/h); — numerical determinations; ● experimental values at the inlet; ■ experimental values at the outlet

Nusselt curves obtained experimentally. The agreement seems to be good (see Figure 11), except for the points corresponding to $T_w < 0^\circ\mathrm{C}$ for which icing appears. The determination of the axial velocity profiles at the exit allows a second comparison and shows the following effect already observed by Scirocco et al. (1985): the fall in the wall temperature causes an increase in the apparent viscosity near the wall, which, therefore, changes the structure of the flow by introducing a radial velocity component directed toward the center of the cylinder. Figures 12 and 13 show that this change is much more important for high wall temperatures, which mainly explains the negative influence of the inlet temperature T_e on the values of the Nusselt numbers.

Influence of an ice deposit. The appearance of an ice deposit may induce a drastic decrease in the transport coefficient (see Figure 11 results pointed out by an arrow). Because we have no means of measuring the deposit

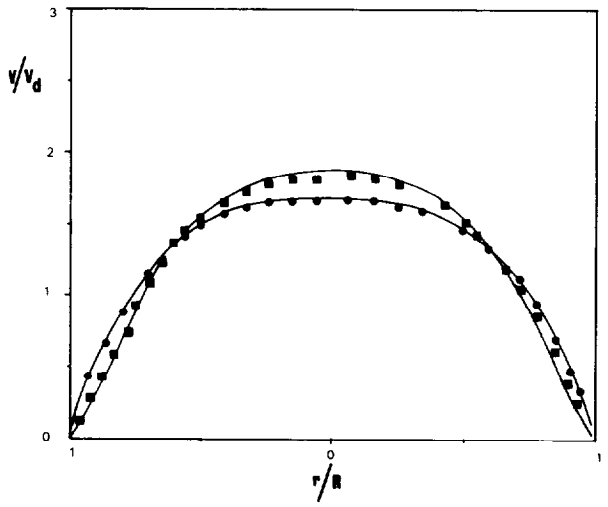

Figure 13 Axial velocity V/V_d evolution (for $T_e = 52°C$, 1.200 1/h); — numerical determinations; ● experimental values at the outlet

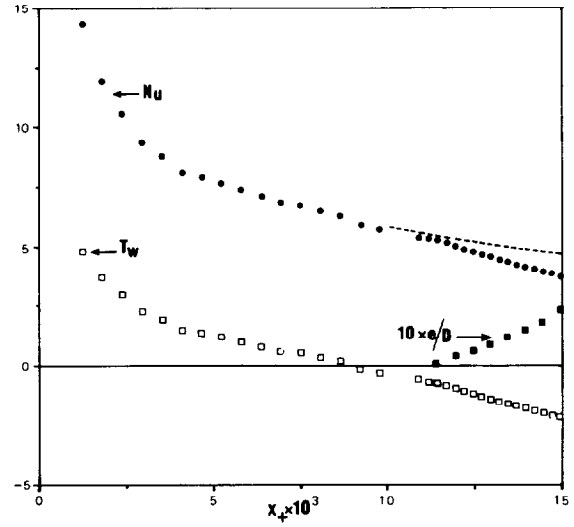

Figure 14 Ice deposit estimation; ● Nusselt number Nu; ---- Nu' analytic continuation of the Nusselt curve; ■ e/D ratio

thickness, we simply propose an estimate, the calculation of which is based on the two following simplifying assumptions.

(1) The temperature of the c.m.c ice interface is at the freezing point (0°C).

(2) The Nusselt number Nu' at this interface has the same value as the one we would obtain for the same dynamical conditions derived from the preceding proposed correlation (this is equivalent to evaluating an analytic continuation of the Nusselt curve). In this case, we have $e = D \cdot \lambda_g/\lambda \cdot (1/\mathrm{Nu} - 1/\mathrm{Nu}')$ where λ_g is the thermal conductivity of ice. Figure 14 demonstrates that the ratio e/D becomes large at the end of the cooled region. These values should be confirmed either by direct measurement or by analyzing the consequent pressure loss.

Conclusion

We have studied the flow of a pseudoplastic material cooled by turbulent counterflow, which is of considerable practical interest. This study has shown that it is possible to determine the local values of the heat transfer coefficient. The evolution of the measured temperature and the calculated flux indicate that we are far from the common assumption that these quantities remain constant. Moreover, it seems necessary to take into account the interaction between the thermal and dynamical fields, which leads to a more complex analysis.

References

Christiansen, E. B., Jensen, G. E. and Tao, F. S. 1966. Laminar flow heat transfer. *AIChE J.*, **12**, 1196–1202

El Ouardighi, A., Van Tuan, N. and Lebouché, M. 1989. Ecoulement et transfert de chaleur par convection forcée pour un fluide non Newtonien thermodépendant. *C.R. Acad. Sci. Paris*, **308**, 91–99

Forest, G. and Wilkinson, W. L. 1977. Laminar heat transfer to power law fluids in tubes with constant wall temperature. *Trans. Inst. Chem. Eng.*, **51**, 331–337

Joshi, S. D. and Bergles, A. E. 1982. Heat transfer laminar flow of non-Newtonian fluids in tubes. *J. Heat Transfer*, **3**, 51–56

Mahalingham, R., Tilton, L. O. and Coulson, J. M. 1975. Heat transfer in laminar flow of non-Newtonian fluids. *Chem. Eng. Sci.*, **30**, 921–929

Metzner, A. B. and Gluck, D. F. 1959. Heat transfer to non-Newtonian fluids under laminar-flow conditions. *Chem. Eng. Sci.*, **12**, 185–190

Metzner, A. B., Vaughn, R. D. and Houghton, G. L. 1957. Heat transfer to non-Newtonian fluids. *AIChE J.*, **3**, 92–100

Mitzushina, T., Ito, R., Kuriwake, Y. and Yahikagawa, K. 1967. Boundary-layer heat transfer in a circular tube to Newtonian and non-Newtonian fluids. *Kagaku-Kogaku Ronbunshu*, **31**, 250–256

Oliver, D. R. and Jenson, V. G. 1964. Heat transfer to pseudoplastic fluids in laminar flow in horizontal tubes. *Chem. Eng. Sci.*, **19**, 115–129

Popovska, F. and Wilkinson, W. L. 1977. Laminar heat transfer to Newtonian and non-Newtonian fluids in tubes. *Chem. Eng. Sci.*, **32**, 1155–1164

Scirocco, V., Devienne, R. and Lebouché, M. 1985. Ecoulement et transfert de chaleur pour un fluide pseudoplastique dans la zone d'entrée d'un tube. *Int. J. Heat Mass Transfer*, **28**, 91–99

Sieder, E. N. and Tate, G. E. 1936. Heat transfer and pressure drop of liquids in tubes. *Ind. Eng. Chem. Research*, **28**, 1429–1435